Journal of Zhejiang University-SCIENCE A (Applied Physics & Engineering)
ISSN 1673-565X (Print); ISSN 1862-1775 (Online)
www.zju.edu.cn/jzus; www.springerlink.com
E-mail: jzus@zju.edu.cn

Development on test equipment of coal slurry mixing tank*

Jin WANG[†1], Xu-wen ZHANG[2], Zhi-ping CHEN[†‡1], Jian-hua LAN[2]

([1]*Institute of Process Equipment, Zhejiang University, Hangzhou 310027, China*)

([2]*Shanghai Research Institute of Chemical Industry, Shanghai 200062, China*)

[†]E-mail: wjzju8606@126.com; zhiping@zju.edu.cn

Received Jan. 8, 2009; Revision accepted July 13, 2009; Crosschecked Jan. 7, 2010

Abstract: A coal slurry mixing tank is a key piece of equipment in the preparation of coal slurry for direct coal liquefaction. It is a gas-liquid-solid three-phase mixing device. Based on the performance of the existing coal slurry mixing equipment, a type of test equipment for horizontal continuous coal slurry preparation was developed, but to this point has limited research results. The test equipment consists of a mixing cylinder, mixer, stirring impeller and other components. Slurry mixing experiments were undertaken using the prototype, testing the performance of the device. A mathematical model was proposed specifically for the operation of a coal slurry mixing tank that is horizontally operated with high slurry concentration and rotary flow. The flow field in the horizontal coal mixing tank was simulated with the computational fluid dynamic (CFD) method. The experimental results match well with the CFD simulation results. Results show that the test device of a coal slurry mixing tank can be used to model the mixing of pulverized coal and the solvent oil. A strong correlation was obtained.

Key words: Gas-liquid-solid mixing, Mixing equipment, Experimental research, Numerical simulation, Direct liquefaction
doi:10.1631/jzus.A0900022 **Document code:** A **CLC number:** TH7; TM15

1 Introduction

Coal liquefaction is an available technology for solving the energy sources all over the world which are contaminative and with lower efficiency. Coal direct liquefaction is done through adding hydrogen into a coal slurry and solvent oil system. This process creates a change in the oil under the functions of high temperature, high pressure, and the activator. The advantage of coal direct liquefaction is high thermal efficiency and high liquid production yield. Contrarily, the operating condition is rigorous. As a key piece of equipment in the initial stage of coal direct liquefaction technology, coal slurry preparation device directly affects the whole process.

Recent mixer research mainly focuses on solid-liquid with vertical double-layer or triple-layer blender (Sherwood, 1987; Wang *et al*., 2003), rarely on gas-liquid-solid mixing flow. Only a few, such as Calabrese *et al*. (2000) from University of Maryland, made further studies and experiments in this area and achieved some computational fluid dynamic (CFD) numerical simulation results.

A horizontal coal slurry mixing tank with gas-liquid-solid phrases was studied and developed with experimental verification and numerical simulation, which is used to mix pulverized coal and solvent oil.

2 Structure design

2.1 Alternative between horizontal and vertical tanks

Usually, solid feed-in are mainly pulverulent particles. Once vertical mixing equipment is employed, heated oil would produce steam, and encumber the solid feed-in process. Worse still, the gas would harm the contact between the crushed solid and liquid medium, leading to a low blender efficiency (Xiao and Takahashi, 2007). To avoid such flaws, a solid-liquid mixing tank has been designed horizontally.

‡ Corresponding author

* Project (No. 2008C21021) supported by the Science and Technology Research Program of Zhejiang Province, China

2.2 Agitator selection

A disc turbine impeller with large shear force enables more efficient liquid micelle dispersion. An Impeller with 45° oblique blade makes the mixture have both the circular and axial velocity components for propulsion (Chen *et al*., 2004). Therefore, a 45° oblique blades disc turbine impeller was chosen.

2.3 Vent design

It is evitable that air will enter into the tank during the feed of pulverized coal. Simultaneously, steam and solvent vapor will be emitted during mixing of the hot solvent oil and pulverized coal with catalyst. All these may lead to bumping, agglomeration of pulverized coal, low conversion rate or even pipe blockage and system shutdown. Additionally, if steam rises up to the pulverized coal feeding system, the agglomeration of dry pulverized coal by moisture will lead to destruction of the coal slurry preparation system. Thus, a vent connecting a vacuum pump at the downstream section of the mixing tank was applied for degasification.

2.4 Design of removable baffles

In this system three removable baffles were adopted, to prevent material between neighboring stirring impeller blades from making direct contact, avoiding dead angle of flow, enhancing turbulence of liquid (Bhattacharya *et al*., 2007; Torre *et al*., 2007), thus obtaining a better mixed effect.

Furthermore, for more convenient installation and maintenance, the mixing tank was designed as a combination of upper cover and lower cover, connected with bolts. For easier cleaning, three openings were set at the bottom of the tank.

3 Operation principle

Pulverized coal and solvent oil feed into the mixing tank through feeding pipes. Raw materials are mixed in the tank under centrifugal force, created by multiple impellers during rotation. Simultaneously, axial space in the horizontal tank is partitioned into several small mixing parts by baffles, which limit material movement in the planned path and range. Mixed materials are discharged from the vent using the effect of the disc turbine impeller for the next procedure (Fig. 1).

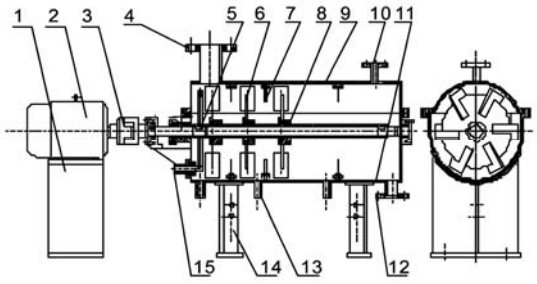

Fig. 1 Structure of coal slurry mixing tank
1: electromotor pedestal; 2: electromotor; 3: joint slack; 4: pulverized coal inlet pipe; 5: liquid inlet annulus pipe; 6: impeller; 7: baffle; 8: revolution axis; 9: cylinder upper cover; 10: gas vent pipe; 11: cylinder below cover; 12: mixture vent pipe; 13: cleaning orifice; 14: mixing tank pedestal; 15: liquid inlet pipe

4 Prototype manufacture and testing system

A coal slurry mixing tank was produced according to the parameters given in Table 1. The pulverized coal is fed by a screw feeder, which has a simple structure and good operational flexibility with control of the rotational speed of screw. Solvent oil is fed by a metering pump, which can control the flow rate of liquid and increase the velocity of fluid entering the mixing tank. Additionally, a screen was installed on the gas vent for preventing solid particles from dropping into the exhaust system. Fig. 2 shows the process flow diagram of the testing system. The locale equipment for testing is shown in Fig. 3.

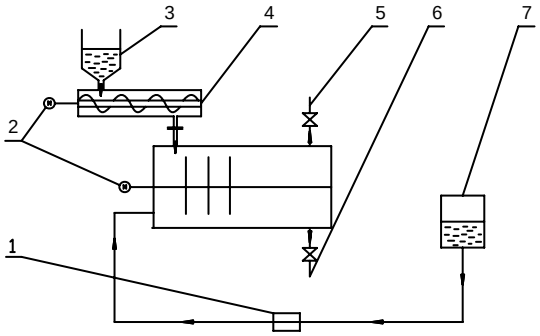

Fig. 2 Process flow of test system
1: metering pump; 2: electromotor; 3: coal scuttle; 4: deposited fixing for coal; 5: vent; 6: sample connection; 7: deposited fixing for oil

5 Testing result and analysis

Table 2 shows the relation between sample time and solid mass percentage composition under the designed condition. In the experiment, the

Table 1 Structure and operation parameters of coal mixing tank

Parameter		Value
Cylinder inner diameter (mm)		261
Pulverized coal inlet pipe diameter (mm)		55
Mixture vent pipe diameter (mm)		25
Gas vent pipe diameter (mm)		15
Mixing axis	Outer diameter (mm)	34
	Rotate speed (r/min)	200
Stirring impeller	Outer diameter (mm)	250
	Oblique angle of blade (rad)	π/4
Impeller blade	Length (mm)	72
	Breadth (mm)	55
	Thickness (mm)	5
Baffle	Inner diameter (mm)	154
	Outer diameter (mm)	261
Solvent oil	Density (kg/m^3)	896
	Dynamic viscosity (Pa·s)	0.0439
	Inlet flux (kg/h)	39.6
Pulverized coal	Stack density (kg/m^3)	450
	Density (kg/m^3)	880
	Dynamic viscosity (Pa·s)	0.8
	Granule diameter (μm)	60
	Inlet flux (kg/h)	40

(a)

(b)

Fig. 3 Locale picture of experimental facility
(a) Experimental facility; (b) Inner structure of mixed tank

homogeneous mixing of materials was considered to be achieved after the errors of total solid mass percents were less than 5% and repeated several times in the same sample time interval. According to Table 2, in the mixing tank mixed material was acquired after 180 operations. It proves that the parameters conform to the design requirement, achieving the homogeneous mixing of pulverized coal and solvent oil.

The average value of total solid mass percentage composition after homogeneously mixing from corresponding values of the sample times from 180 s to 600 s was 45.75%.

Table 2 Solid mass percentage composition vs. sampling time

Sample time (s)	Solid mass (%)	Sample time (s)	Solid mass (%)
20	10.50	390	45.43
60	26.87	480	47.21
180	43.63	540	47.77
240	44.14	600	48.06
300	44.07		

6 Numerical simulation

To investigate more about internal fluid flowing process and compare it with test data, the CFD method was introduced to simulate flowing process with software Fluent 6.2 (Guha *et al*., 2007). Due to the radius of the upper and lower parts of the mixing tank's main bulk, whole mixing tank was regarded as a cylinder in modeling. The vacuum state and cleaning pipe were ignored and the internal area surrounded by the walls of mixing tank, rotary axis, stirring impellers, baffles and access pipes was covered in this model (Guha *et al*., 2008; Delafosse *et al*., 2008).

6.1 Control equations

The rotation speed of the mixer shaft is 200 r/min. The rotating flow of mixed liquid is considered to be a turbulent motion, as its Reynolds number Re>>4000. Based on multiphase flow mechanism, the control equations consist of a quality equation, momentum equation, renormalization-group (RNG) k-ε equations and component conservation equation (Guevara *et al*., 2008), where the quality conservation equation is

$$\frac{\partial u_i}{\partial x_i}=0. \tag{1}$$

Momentum conservation equation is

$$\begin{aligned}&\frac{\partial(\rho u_i u_j)}{\partial x_j}+\frac{\partial(\rho u_i)}{\partial t}\\&=\frac{\partial}{\partial x_j}\left[\mu\left(\frac{\partial u_i}{\partial x_j}+\frac{\partial u_j}{\partial x_i}-\frac{2}{3}\delta_{ij}\frac{\partial u_t}{\partial x_t}\right)\right]-\frac{\partial p}{\partial x_i}+\frac{\partial(-\overline{\rho u_i' u_j'})}{\partial x_j}.\end{aligned} \tag{2}$$

RNG k-ε equations are

$$\begin{aligned}&\frac{\partial}{\partial t}(\rho k)+\frac{\partial}{\partial x_i}(\rho k u_i)\\&=\frac{\partial}{\partial x_j}\left(\alpha_k\mu_{\text{eff}}\frac{\partial k}{\partial x_j}\right)+G_k+G_b-\rho\varepsilon-Y_M+S_k,\end{aligned} \tag{3}$$

$$\begin{aligned}&\frac{\partial}{\partial t}(\rho\varepsilon)+\frac{\partial}{\partial x_i}(\rho\varepsilon u_i)\\&=\frac{\partial}{\partial x_j}\left(\alpha_\varepsilon\mu_{\text{eff}}\frac{\partial\varepsilon}{\partial x_j}\right)+C_{1\varepsilon}\frac{\varepsilon}{k}(G_k+C_{3\varepsilon}G_b)\\&\quad-C_{2\varepsilon}\rho\frac{\varepsilon^2}{k}-R_\varepsilon+S_\varepsilon,\end{aligned} \tag{4}$$

with

$$G_k=-\rho\overline{u_i'u_j'}\frac{\partial u_j}{\partial x_i},\ G_b=\beta g_i\frac{M_t}{Pr_t}\frac{\partial T}{\partial x_i},$$

$$Y_M=2\rho\varepsilon M_t^2,\ \mu_t=\rho C_\mu\frac{\kappa^2}{\varepsilon},$$

$$R_\varepsilon=\frac{C_\mu\rho\eta^3(1-\eta/\eta_0)\varepsilon^2}{(1+\beta\eta^3)k},\ \eta=\frac{S_k}{\varepsilon}.$$

Component conservation equation is

$$\frac{\partial(\rho c_s)}{\partial t}+\text{div}(\rho u c_s)=\text{div}[D_s\text{grad}(\rho c_s)]+S_s. \tag{5}$$

In Eqs. (1)–(5), δ_{ij} is Kroneker sign; ρ is the density of liquid, kg/m^3; g is acceleration of gravity, m/s^2; k is the energy of turbulent motion, m^2/s^2; ε is the dissipation rate of turbulent motion, m^2/s^3; G_k is turbulence energy caused by laminar velocity grads; G_b is turbulence energy caused by buoyancy; Y_M is wave motion caused by excessive spread; S_ε and S_k are defined by user; $C_{1\varepsilon}$, $C_{2\varepsilon}$ and $C_{3\varepsilon}$ are the constants of k-ε model; u is the velocity component, m/s; μ is coefficient of kinetic viscosity, Pa·s; α_k and α_ε are the Prandtl number of k and ε equations; β is coefficient of thermal expansion; Pr_t is Prandtl number of turbulent energy; M_t is Mach number of turbulence; C_μ is constant of model; c_s is volume fraction of component s; D_s is diffusion coefficient of component s; and S_s is new component get in unit time and volume; η_0=4.38, β=0.012.

6.2 Inlet and outlet boundary conditions

Generally, there are three methods to define inlet boundary conditions, namely pressure, velocity and flux. If the inlet is near the solid wall in the region needing a solution, it will lead to extremely uneven total pressure distribution in inlet region. Therefore, the pressure inlet boundary is not fit for this model. The flux and velocity boundaries have the same function for incompressible fluid, therefore, the velocity boundary was chosen and we assume inlet velocity to be distributed uniformly.

Since the condition of mixture and gas outlet was unknown, pressure outlet (1.0×10^5 Pa) was chosen and then defined as only mixture with coal. Solvent oil came from the mix-outlet and only gas came from the gas-outlet.

6.3 Convergence criteria

The absolute accumulative error of the whole field was used for estimating whether the result was convergent or not (Murthy *et al*., 2007). The absolute error of the k time iterative is

$$R_\Phi^k=\frac{\sum\left|\boldsymbol{A}_p\boldsymbol{\Phi}_p^k-\sum_m\boldsymbol{A}_m\boldsymbol{\Phi}_m^k-s_1\right|}{\sum_p\boldsymbol{A}_p\boldsymbol{\Phi}_p^k}, \tag{6}$$

where n is iteration number; $\boldsymbol{A}_p$ is p dimension coefficient matrix; $\boldsymbol{A}_\text{m}$ is m dimension coefficient matrix; $\boldsymbol{\Phi}_p$ is p dimension vector; $\boldsymbol{\Phi}_\text{m}$ is m dimension vector; and s_1 is experience error. When the absolute error in calculation is below the point, the result is considered to be constringency. The convergent target is $\max(R_\Phi^k)\le1.0\times10^3$.

7 Simulation result analysis

7.1 Distribution of turbulent motion in longitudinal cross section

Fig. 4 is the distribution nephogram of turbulent flow intensity in section z=0. Because of the centrifugal force, in the parts where the radial distance is large, there is a comparatively high turbulent intensity of liquid. Turbulent intensity near baffles is higher than that of other areas and it begins to decrease when the fluid reaches the blades. Taking no account of access pipes, the bubble is formed near the wall of slot between baffle plates and blades, where the maximum turbulent flow intensity appears. The phenomena above demonstrate that baffles play an important part in enhancing the turbulence of liquid and well-mixing coals and oils.

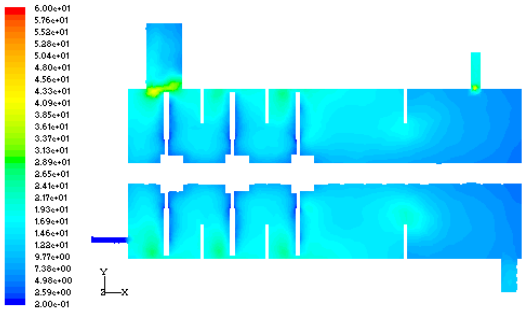

Fig. 4 Distribution of turbulent flow intensity in section z=0

7.2 Distribution of internal speed

Fig. 5 describes the speed vector near rotate wall. The speed is in direct proportion to the arrowheads of the speed vector, which indicates the whole rotary trend. Due to the rotary centrifugal force, the liquid near blades reaches a higher speed than the one near mixer shaft. Liquid not only has a circular component velocity but also has axial component velocity with 45° oblique turbine impeller, namely it makes a complex motion involving both a circular motion around the central axis and an axial translation.

Fig. 6 describes the flow line in section z=0. It indicates that there were a few bubbles beside baffles which could indicate the equality mix of oil and coal which avoids flowing dead angle and reduce material cumuli.

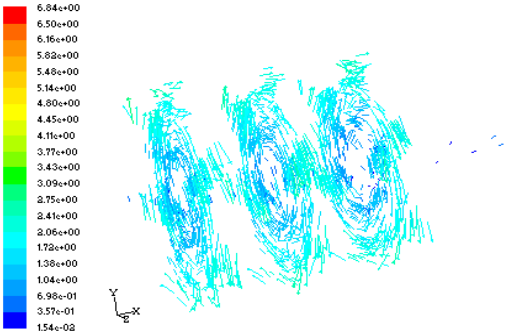

Fig. 5 Distribution of speed vector nearby rotate wall

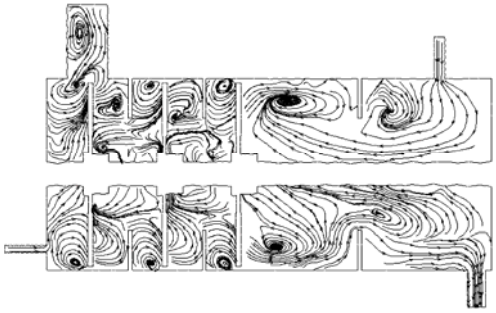

Fig. 6 Distribution of flown line in section z=0

7.3 Analysis of mixing effect under design conditions

Fig. 7 denotes the volume fraction distribution of oil and coal in the outlet section. Currently, if the volume fraction of every phase in the outlet section fluctuates below 1%, the material is considered to be mixed well. The chart shows that volume fraction of coal fluctuates between 4.282% and 4.290% and that of oil between 4.297% and 4.307%. In the whole outlet section, the volume fractions of coal and oil remain almost invariant and the largest fluctuant range which is accords with the point of the original proportion meaning that coal and oil have already mixed to 0.01%, and is placed well. The average volume fractions of the coal and oil in the outlet mixture are respectively 4.286% and 4.302%. By changing it into mass percentage composition the solid mass percentage composition can be computed as 49.5%.

8 Conclusion

8.1 Internal flow characteristic

During the operation of the test equipment, vorticity usually appears between the baffle plates and

impellers under the action of disc turbine impeller. This not only helps to prevent the stacking of materials in the baffle plate and production of a dead angle but also makes pulverized the coal and solvent oil mix more uniform.

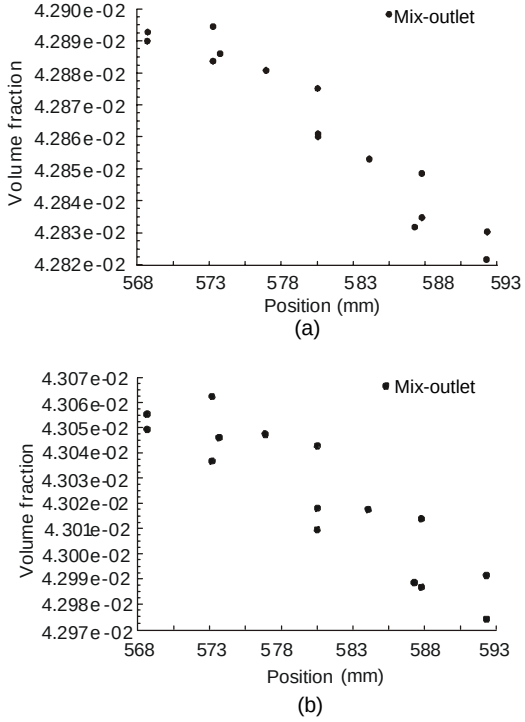

Fig. 7 Volume fraction distribution of (a) coal and (b) oil in outlet section

8.2 Comparison between simulation and experimental results

The error between numerical simulation and experimental result is shown below:

$$\frac{49.5-45.75}{45.75}\times 100\% = 8.2\%.$$

The error can be constructed to be under 10%, which is the permissible engineering error. By comparison with the results above, it can be concluded that the design meets the technical requirements very well.

8.3 Expectation

This paper studied the process of the lab-scaled equipment, but the real industrialized coal slurry mixing tank size is much larger than this one. Therefore, further larger research is required.

References

Bhattacharya, S., Hebert, D., Kresta, S.M., 2007. Air entrainment in baffled stirred tanks. *Chemical Engineering Research and Design*, **85**(5):654-664. [doi:10.1205/cherd06184]

Calabrese, R.V., Francis, M.K., Mishra, V.P., Phongikaroon, S., 2000. Measurement and Analysis of Drop Size in Batch Rotor-stator Mixer. Proceedings of 10th European Conference on Mixing. Elsevier Science BV, Delft, p.149-156.

Chen, Z.P., Zhang, X.W., Lin, X.H., 2004. Preferred Manual of Stirring and Mixing Devices. Chemistry Industry Publishing Company, p.108-115 (in Chinese).

Delafosse, A., Line, A., Morchain, J., Guiraud, P., 2008. LES and URANS simulations of hydrodynamics in mixing tank: Comparison to PIV experiments. *Chemical Engineering Research and Design*, **86**(12):1322-1330. [doi:10.1016/j.cherd.2008.07.008]

Guha, D., Ramachandran, P.A., Dudukovic, M.P., 2007. Flow field of suspended solids in a stirred tank reactor by Lagrangian tracking. *Chemical Engineering Science*. **62**(22):6143-6154. [doi:10.1016/j.ces.2007.06.033]

Guha, D., Ramachandran, P.A., Dudukovic, M.P., 2008. Evaluation of large eddy simulation and euler-euler CFD models for solids flow dynamics in a stirred tank reactor. *AIChE Journal*, **54**(3):766-778. [doi:10.1002/aic.11417]

Guevara, L.E., Sanjuan, G.R., Cordova, A.M., Soledad, C.G., Ascanio, G., Galindo, E., 2008. High-speed visualization of multiphase dispersions in a mixing tank. *Chemical Engineering Research and Design*, **86**(12):1382-1387. [doi:10.1016/j.cherd.2008.07.013]

Murthy, B.N., Ghadge, R.S., Joshi, J.B., 2007. CFD simulations of gas-liquid-solid stirred reactor: Prediction of critical impeller speed for solid suspension. *Chemical Engineering Science*, **62**(24):7184-7195. [doi:10.1016/j.ces.2007.07.005].

Sherwood, R., 1987. A Blender Used for Mixing Slurry Material and Liquid or Double-state. China Patent No. CN87102245 (in Chinese).

Torre, J.P., Fletcher, D.F., Lasuye, T., Xuereb, C., 2007. Single and multiphase CFD approaches for modelling partially baffled stirred vessels: Comparison of experimental data with numerical predictions. *Chemical Engineering Science*, **62**(22):6246-6262. [doi:10.1016/j.ces.2007.06.044]

Wang, F.D., Wang, Z.N., Rui, S., 2003. A Device Producing Coal-water or Coal-coil Slurry. China Patent No. CN2644909Y (in Chinese).

Xiao, H.H., Takahashi, K., 2007. Mixing characteristics in the horizontal non-baffled stirred vessel in low viscosity fluid. *Journal of Chemical Engineering of Japan*, **40**(8):679-683. [doi:10.1252/jcej.40.679]